Comparison of parametrization techniques for an electrical circuit model of Lithium-Sulfur batteries

5 authors, including:

Vaclav Knap
Aalborg University

18 PUBLICATIONS   **34** CITATIONS

SEE PROFILE

Daniel-Ioan Stroe
Aalborg University

59 PUBLICATIONS   **234** CITATIONS

SEE PROFILE

Remus Teodorescu
Aalborg University

117 PUBLICATIONS   **632** CITATIONS

SEE PROFILE

Some of the authors of this publication are also working on these related projects:

Project   Capacitor voltage ripple reduction and arm energy balancing in MMC-HVDC View project

Project   Intelligent and Efficient Power Electronics View project

Aalborg Universitet

Comparison of Parametrization Techniques for an Electrical Circuit Model of Lithium-Sulfur Batteries

Knap, Vaclav; Stroe, Daniel Loan; Teodorescu, Remus; Swierczynski, Maciej Jozef; Stanciu, Tiberiu

Comparison of Parametrization Techniques for an Electrical Circuit Model of Lithium-Sulfur Batteries

Vaclav Knap, Daniel-Ioan Stroe, Remus Teodorescu, Maciej Swierczynski, and Tiberiu Stanciu

Department of Energy Technology, Aalborg University, Denmark

Email: vkn@et.aau.dk

Abstract—**Lithium-Sulfur (Li-S) batteries are an emerging energy storage technology, which draw interest due to its high theoretical specific capacity (approx. 1675 Ah/kg) and theoretical energy density of almost 2600 Wh/kg. In order to analyse their dynamic behaviour and to determine their suitability for various commercial applications, battery performance models are needed. The development of such models represents a challenging task especially for Li-S batteries because this technology during their operation undergo several different chemical reactions, known as polysulfide shuttle. This paper focuses on the comparison of different parametrization methods of electrical circuit models (ECMs) for Li-S batteries. These methods are used to parametrize an ECM based on laboratory measurements performed on a Li-S pouch cell. Simulation results of ECMs are presented and compared against measurement values and the accuracy of parametrization methods are evaluated and compared.**

I. INTRODUCTION

Lithium-Sulfur (Li-S) batteries belong to a recently hot discussed topic among the emerging battery technologies. It is due to their high theoretical specific capacity and theoretical energy density, which would result in a decreased weight of battery cells. Furthermore, the sulfur abundance decreases the battery manufacturing cost in comparison to metals used in lithium-ion batteries and it is as well more environmentally friendly [1].

Nowadays, Li-S batteries become commercially available, even though their performance is still far from their theoretical limits. For analysing their performance at different conditions (e.g. temperature, state-of-charge (SOC) or current), there is a need for an accurate battery performance model. Moreover, this performance model may be required to run online in certain applications and in this case it needs to have a fast computation time. All these requirements can be met by an equivalent circuit model (ECM). Moreover, ECMs are based on basic electrical components (e.g. voltage sources, resistors etc.), which can be easily integrated into a complex model, e.g. an electric vehicle [2]–[4].

An important task for developing the specific ECM of a battery is to parametrize it. At first, the appropriate measurements have to be performed. The widely used measurement methods for parametrizing an ECM are electrochemical impedance spectroscopy (EIS) [5] or current pulse-based methods [6], [7]. The next step is the selection of the ECM topology, which is followed by the estimation of the parameters from the measurement data. Researchers have proposed different

methods, which are dealing with this task by means of different parametrization approaches [5], [7]–[14]. In the literature, mainly the determination of ECM's parameters based on the EIS measurements have been used for the Li-S batteries [15], [16]. Identification of the parameters from current pulse-based measurements for a Li-S battery has been so far used only in [17]; however, the parametrization technique has not been specified.

This paper gives an overview of different parametrization methods for a Li-S battery ECM. These methods are applied to a Li-S pouch battery cell and in consequence, the ECM parameters are estimated. Finally, simulations for the obtained ECMs are performed and the parametrization techniques are evaluated and compared.

The paper is structured as follows: Section II describes briefly fundamentals of Li-S batteries. Afterward, in Section III, there is introduced an ECM for Li-S batteries. The measurement methods for parametrization of the proposed ECM and parametrization techniques are presented in Section IV. Thus, it is followed by the description of an experiment and results in Section V and the discussion of obtained results in Section VI. Conclusions and future work are summarized in Section VII.

II. LITHIUM-SULFUR BATTERIES

The Li-S battery is composed of a sulfur compound cathode, an electrolyte (polymer or liquid), and a lithium anode. Furthermore, different additives and binders can be added in order to improve the battery's characteristics. Sulfur is a perspective cathode material, which offers a high theoretical specific capacity of approximately 1675 mAh/g. Moreover, the theoretical energy density of a Li-S battery is approx. 2600 Wh/kg, which is five times more than the theoretical energy density of Lithium-ion (Li-ion) batteries. The basic Li-S redox reaction is written as [18]:

$$16Li + S_8 \longrightarrow 8Li_2S. \tag{1}$$
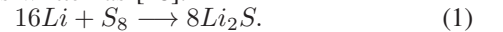
However, the internal chemical processes of the Li-S battery are more complex than in the case of commercial Li-ion batteries. The reduction of sulfur from S_8 to S is a multi-stage process during which different types of polysulfides (Li_2S_n) are formed and dissolved. In Fig. 1, there is shown the typical discharge voltage profile for a Li-S battery and four stages are illustrated, together with their corresponding dominant chemical reactions [18]. During the reverse operation (charging),
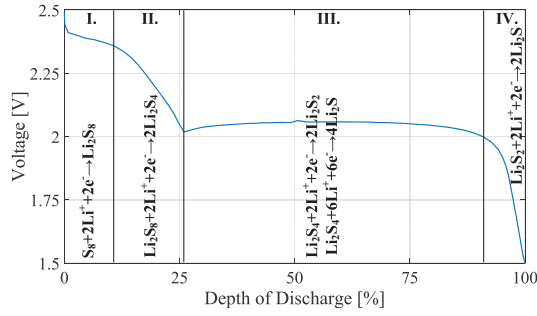
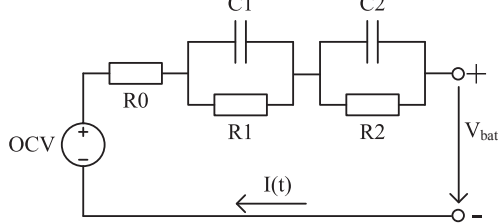Fig. 1. Voltage profile of a Li-S cell during discharging.

Fig. 2. An electrical circuit model for a Li-S battery cell.

Fig. 3. Measured impedance spectra of a Li-S cell.

the polysulfides with a shorter chain length are oxidized and recombined to polysulfides with a longer chain length. This process of polysulfide circulation is known as a polysulfide shuttle.

The polysulfides with a longer chain length are vastly soluble in frequent liquid organic electrolytes. However in the case of the polysulfides Li_2S and Li_2S_2, their insolubility in the organic electrolytes causes their sedimentation on the anode surface and in areas of the cathode, which are electronically insulated. In this way, the sedimented Li_2S/Li_2S_2 do not participate anymore in the charging and discharging of the battery. Consequences of the polysulfide shuttle are an increased internal battery resistance, fast capacity degradation, low coulombic efficiency, and high self-discharge. Therefore, one of the scientific focus is to avoid these negative effects of the polysulfide shuttle. Nevertheless, the polysulfide shuttle has also a positive effect, which is an inherent protection against cell overcharge [1].

III. A LITHIUM-SULFUR BATTERY ECM

The ECM used in this work is based on the equivalent circuit proposed in [19] for a Li-S cell in an intermediate state. For the ECMs parametrized based on EIS measurements, constant phase elements (CPEs) are usually used instead of capacitors to take into account a non-ideal behaviour of the electrode, like a roughness of the surface and porosity of a material [20]. However, if the parametrization is performed based on current pulse measurements, then, the utilized model contains only capacitors instead of CPEs. The layout of the ECM used in this work for modeling the dynamic behaviour of the Li-S cell is presented in Fig. 2. According to [19], R_0 represents the electrolyte resistance, R_1 stands for the total surface layers resistance of the sulfur and lithium electrodes, C_1 is the distributed surface layers capacitance on both electrodes, R_2 expresses the charge transfer resistance on the sulfur electrode and C_2 interprets the double layer capacitance distributed on the surface of the pores in the sulfur electrode.
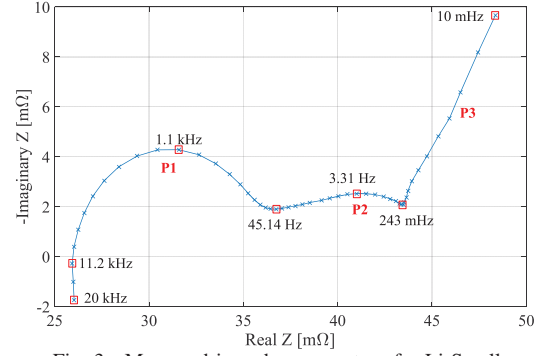
IV. MEASUREMENT AND PARAMETRIZATION TECHNIQUES

There are two types of widely used measuring methods, which provide input data for parametrizing of ECMs: the EIS and the current pulse-based methods.

A. EIS Measurements

EIS was firstly used as a method for characterizing the electrical attributes of materials. The measurement technique is based on applying a sinusoidal voltage or current and measuring the phase shift and amplitude of the non-applied signal in order to obtain the AC impedance relevant to the applied frequency. Usually, multiple frequencies are considered during the measurement and the final result is the impedance spectrum of the battery cell [5]. The spectrum is graphically presented as a Nyquist plot, as it is shown in Fig. 3 for a Li-S battery. In Fig. 3, there are marked phases of the Li-S battery, where according [16]: P1 is caused by the charge transfer of sulfur intermediates, P2 comes from the formation and dissolution of S_8 and Li_2S, and P3 represents diffusion processes.

The EIS can be applied to the battery during a relaxation period [15], [21]. The obtained data are in that case exactly for the specific level of SOC, however it does not reflect the battery parameters dependence on different C-rates. Another option is to superimpose a charging or discharging current during the EIS measurement [22]. This allows for including battery impedance dependence on the charging/discharging battery current. In this case, the battery state is not stationary and the measurement has to be sufficiently fast in order to be valid to a certain level or range of SOC. In [21], an alternative EIS measurement method is presented by applying a superimposed current pulses.

In order to obtain values of the ECM elements, the Nyquist plot is fitted commonly by using a complex nonlinear least squares fitting method [5]. Specialized softwares allow to fit the data to different topologies of ECMs, e.g. ZView software is used in [15]. Nevertheless, in this work the EIS technique was not used to parametrize the ECM.

B. Current Pulse Measurements

Methods based on DC current pulses are divided into two types. The first type is a hybrid pulse power characterization (HPPC) test [6]. The HPPC method consists of a procedure, when the battery is brought to a desired SOC level and is
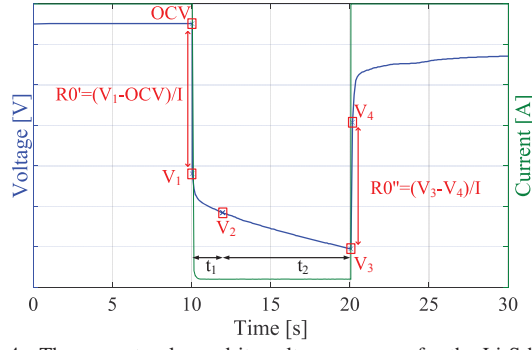
Fig. 4. The current pulse and its voltage response for the Li-S battery.

left for a certain period of time to relax and achieve thermo-dynamic stability. After the relaxation period, a short charging or discharging current pulse is applied and another relaxation period follows before a second current pulse of opposite orientation is applied. It is again followed by the relaxation period. Afterward, the battery is recharged to the new SOC and the steps are repeated for the whole SOC interval. The typical length of the current pulse is 10 seconds [6]; alternatively, a current pulse of 18 seconds can be used [23]. The voltage response of a LiS battery to 10 second current pulse is shown in Fig. 4. Therefore, the SOC during the pulse is usually assumed to be constant; however this assumption may introduce some model inaccuracy, especially for high current pulses.

The second pulse-based method is referred to as galvanostatic intermittent titration technique (GITT) [24]. It consists of constant current pulses in one direction, during which the SOC is shifted to a new level, and of relaxation periods between them. The current pulses do not have to be equally long. For example, battery regions with high voltage dynamics are measured with pulses shifting the SOC about 1%. For more stable voltage regions, the applied current pulses may change the SOC about 10% [7], [25].

C. Parameterization methods based on pulse measurements

Several procedures are proposed in literature for deriving the parameters of the ECMs from pulse measurements. They use the voltage response data during the current pulse [8]–[10] or during the relaxation period after finishing the pulse [7], [11], or they combine both approaches [12].

In references [8], [9], there is described a method that uses the Battery Parameter Estimator Spreadsheet, which is based on a multiple linear regression of measured HPPC data. The process of data fitting is performed manually by using an MS Excel spreadsheet and it is described only for an ECM with one R-C element. This methods is further improved in [9] by using Matlab/Simulink parameter estimation tool and it is referred to as Simulink Parameter Estimation Method. The improved method is supposed to be more accurate and faster; moreover it is suitable for any ECM structure.

The method presented in [10], was originally proposed for the ECM with two R-C elements and it uses the HPPC method applied to a Li-ion battery with current pulse lengths of 10 seconds. Four voltage points are identified during the voltage response under the applied current, as shown in Fig. 4;

they are the open-circuit voltage (OCV), the instantaneous voltage drop after applying the current (V_1), the voltage at 2 seconds (fast dynamics) (V_2) and the voltage at 10 seconds (slow dynamics). From the considered voltage values the ECMs parameters are computed as:

$$R_0 = (OCV - V_1)/I \tag{2}$$
$$R_1 = (V_1 - V_2)/I \tag{3}$$
$$R_2 = (V_2 - V_3)/I \tag{4}$$
$$\tau_1 = R_1 C_1 \tag{5}$$
$$\tau_2 = R_2 C_2 \tag{6}$$

Afterwards, the battery voltage is simulated and compared with the measurements:

$$V_s(t) = OCV + I(t)R_0 + I(t)R_1(1 - e^{-\frac{t}{\tau_1}}) +$$
$$+ I(t)R_2(1 - e^{-\frac{t}{\tau_2}}) \tag{7}$$
$$LSE = (V_{meas}(t) - V_s(t))^2 \tag{8}$$

where $V_s(t)$ is the simulated voltage, $V_{meas}(t)$ is the measured voltage, $I(t)$ is the applied current, t is the time, LSE is the squared error, which is going to be minimized, and τ_1 and τ_2 represents time constant of fast and slow dynamics, respectively. The ECMs parameters are optimized by using the unconstrained optimisation algorithm $fminsearch$ (Nelder-Mead) in Matlab to minimize the error.

The next method, proposed in [7], identifies time constants from the relaxation voltage. The voltage during relaxation, after the initial voltage drop, is expressed as:

$$u_{relax} = OCV - \sum_{i=1}^{n} U_i e^{-\frac{t}{\tau_i}} \tag{9}$$

where u_{relax} is the voltage during relaxation period, U_i is the polarization voltage of ith R-C branch and τ_i is the time constant of the ith R-C branch. Each ith time constant is estimated according:

$$\hat{\tau}_i = \frac{t_{i2} - t_{i1}}{ln(\frac{u_\tau(t_{i1})}{u_\tau(t_{i2})})} \; for \; u_\tau \neq 0 \tag{10}$$

where a hat is used for an estimated value, i stands for the number of the R-C branch, t_{ix} are time coordinates, illustrated in Fig. 5, and u_τ is the transient circuit voltage. The algorithm starts from the longest time constant and proceeds to the shortest one. The assumption is that the time constants have different time scales. The time gap between time windows for a longer and a shorter time constant should be at least three times the value of the shorter time constant, the illustration is shown in Fig. 5. It ensures a negligible influence of the shorter constant branch voltage to the longer time constant parameter extraction, as the voltage of the shorter constant branch dropped under 5% of its initial value. At each step, the transient voltage for the specific time constant is estimated and it is subtracted from the transient voltage for the following time constant identification. The resistance R_i of the ith R-C element is extracted through:

$$R_i = \frac{\hat{U}_i}{I_{cp}(1 - e^{-\frac{t_{cp}}{\hat{\tau}_i}})}, \tag{11}$$
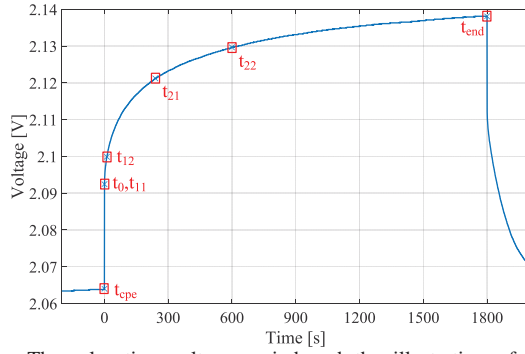
Fig. 5. The relaxation voltage period and the illustration of the point determination for two time constants.

where I_{cp} is the amplitude of the current pulse and t_{cp} is the duration of the pulse. C_i is obtained as follows:

$$C_i = \frac{\hat{\tau}_i}{R_i} \qquad (12)$$

The method can be applied to an ECM with n-combinations of R-C elements.

The other methods presented in [11], [12], [26], do not preliminarily separate the fast and slow time constants from the voltage profile. In one of them, a genetic algorithm is used to find the best result of an applied regression equation; however the time constants have to be approximately known in advance in order to run the regression algorithm [26]. Alternatively, the measured data are fitted to an equation describing the voltage, with preliminary computation of a series resistor, and optimized by a least-square error method [11], [12].

V. EXPERIMENT DESCRIPTION

Laboratory measurements were performed on a Li-S pouch cell supplied by OXIS Energy with a nominal capacity of 3.4 Ah. The cell test connection is shown in Fig. 6, the temperature in the climatic chamber was set to 35° C. At first, two full cycles (0.1 C CHA, 0.2 C DCH) were performed between 2.45 V (SOC=100%) and 1.5 V (SOC=0%). From the second cycle, the reference discharge capacity of 2.918 Ah was measured and the capacity values corresponding to 2.5% and 5% SOC steps were computed accordingly. The GITT was performed with a discharging current of 0.2 C and 30 minutes relaxation time between the pulses, with exception of 1.5 minutes for 100% SOC, 8 minutes for 95%, 15 minutes for 90% and 21 minutes for 85%, as it is shown in Fig. 7. The first pulse at 100% SOC lasted only 18 seconds in order to be able obtain discharging parameters for this SOC level. The OCV was derived from the relaxation period. For high SOC levels (i.e. 100-85%), the cell reached the relaxed state, which is considered as the point where the influence of recovery phase is equal to the influence of self-discharge. Therefore, as the OCV value was considered to be maximal voltage, as illustrated in Fig. 7. For the lower SOC levels (i.e. 80% and less), 30 minutes period was not enough to reach fully relaxed stage. For these cases, the voltage at the end of relaxation period was used for the OCV value. The obtained OCV versus SOC curve is presented in Fig. 8.

The three previously described parametrization techniques were applied to the measured data.. Afterward, the GITT
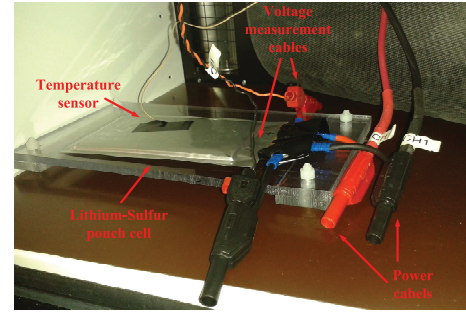

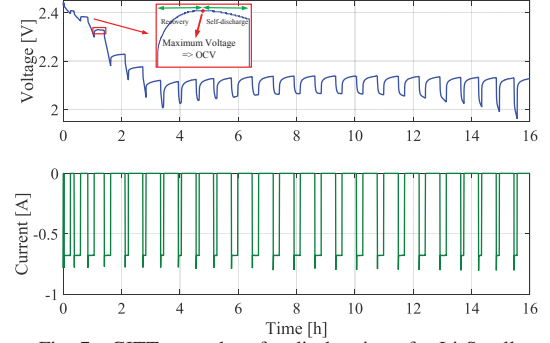Fig. 6. Illustration of the Li-S battery cell during laboratory measurements.

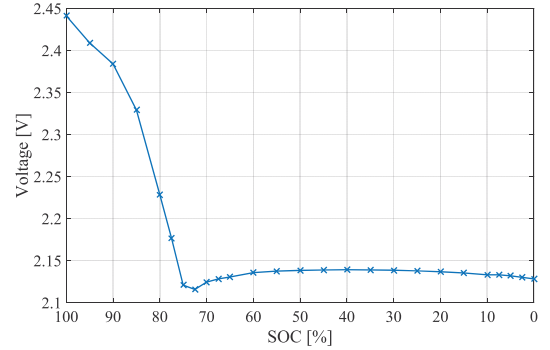Fig. 7. GITT procedure for discharging of a Li-S cell.

Fig. 8. Open circuit voltage of the Li-S cell derived from the relaxation voltage of GITT for discharging steps with 0.2 C-rate.

current profile, shown in Fig. 7, is applied to the parametrized battery model and the resulting voltage profile is compared to the measured one and the sum-of-squared-errors (SSE) (13) is evaluated.

$$SSE = \sum ((V_{meas}(t) - V_s(t))^2) \qquad (13)$$

A. Parametrization Technique 1 (PT1)

The PT1 follows the procedure described in [10]. At first, the original time coordinates were used for 10 seconds current pulse. This case is labeled as PT1a. The time measurement points are presented in Table I. For the optimization, six iteration steps were used as a good compromise between the consistency of trend in parameters and the minimum value of the optimize function. The simulation with one second resolution of GITT profile with the parameters obtained by PT1a has a SSE of 23.35.

For PT1b, the current pulse time window was expanded to 18 seconds, according to [23]. It resulted in the GITT simulation with a SSE of 19.49. The obtained parameters of the ECM for PT1 are shown in Fig. 9.

TABLE I
THE INPUT VOLTAGE POINTS FOR THE PT1. THE CURRENT PULSE STARTS
AT T = 0 S.

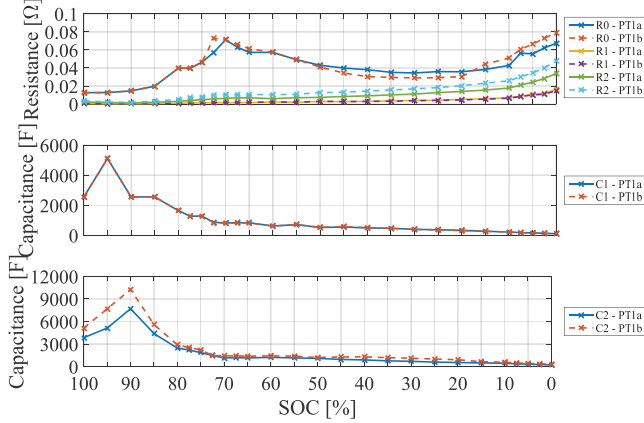| Voltage Point [V]	Time [s]	
	a	b
V_0	0	
V_1	0.5	
V_2	1.5	1.5
V_3	10	18

Fig. 9. PT1: Estimated values for the circuit elements.

TABLE II
THE COORDINATES FOR TIME WINDOWS SELECTION.

SOC level →	100%	95%	90%	85%	≤80%
Time point ↓	Time [s]				
t_{11}	0	0	0	0	0
t_{12}	0.5	2.5	12	12	12
t_{21}	1	7.5	60	120	240
t_{22}	1.5	20	100	300	600
t_{end}	9	58	246	630	1800

B. Parametrization Technique 2 (PT2)

The PT2 follows the methodology presented in [7]. R_0 was computed from the instantaneous voltage drop after the current interruption as shown in Fig. 4. The time windows for two time constants were selected as in the original paper [7]. However, the values for the high SOC levels (85-100%) were adjusted, as the relaxation time for them is shorter. The selected time values are presented in Table II.

Due to the too short time of relaxation period, the parameters for 100% SOC, except R_0 were not estimated. Therefore, their values were extrapolated. By comparing the GITT measurement results with the simulated results, when parametrization technique PT2 was used, returned a SSE of 0.65.

Additionally, *fminsearch* optimization in Matlab, as in the PT1 case, was applied to these parameters (R_1, C_1, R_2, C_2, U_1 and U_2). The previously obtained values were used as initial points and 25 iteration steps were considered. The GITT simulation with these updated parameters decreased the SSE to 0.62. The extracted parameters by PT2 are shown in Fig. 10.

C. Parametrization Technique 3 (PT3)

The PT3 is based on [12]. R_0 was computed in the same way as in PT2, from the current interruption. The function
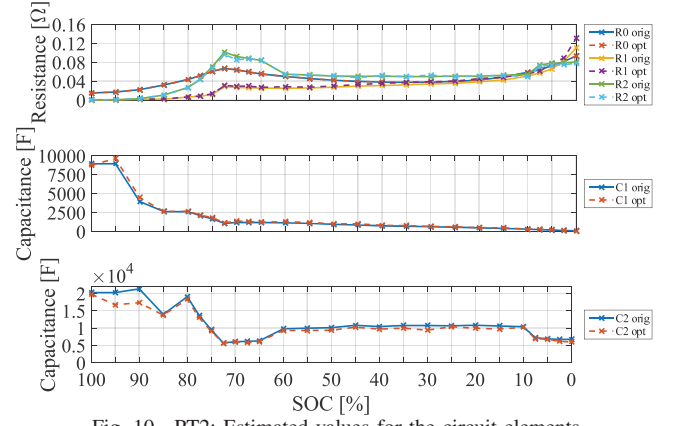

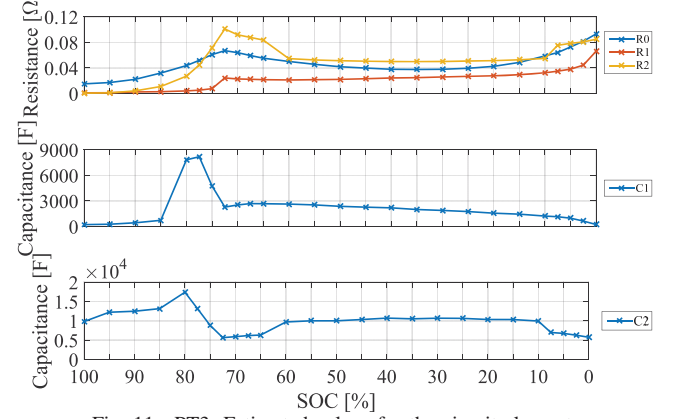Fig. 10. PT2: Estimated values for the circuit elements.
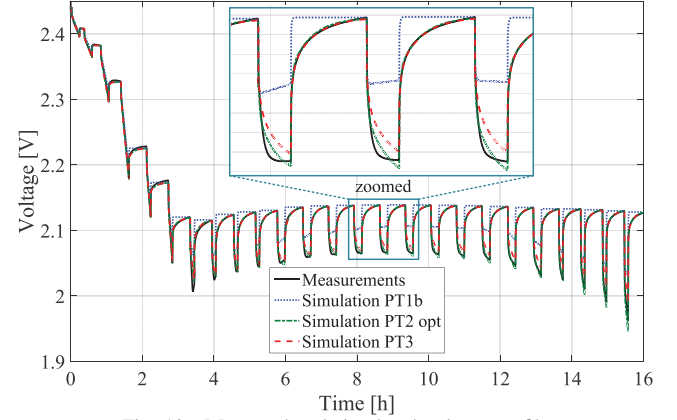

Fig. 11. PT3: Estimated values for the circuit elements.

Fig. 12. Measured and simulated voltage profile.

for the relaxation voltage without the instantaneous drop is described as:

$$V(t) = OCV(SOC) - (U_1 exp^{-t/\tau_1} + U_2 exp^{-t/\tau_2}) \quad (14)$$

The measured relaxation voltage was fitted into (14) by Least Squares method to estimate U_1, U_2, τ_1 and τ_2. The specific R_i and C_i parameters were obtained by solving (11) and (12). The obtained parameters are shown in Fig. 11. In this case, a SSE equal to 1.93 was obtained.

The voltage profiles from the measurement and the ECM simulations (using different parametrization techniques) are presented in Fig. 12.

VI. Discussion

From the simulations, considering an GITT profile, it is visible that PT1 was the less suitable technique for parametrization of the ECM model of a Li-S battery, as it had the significantly largest SSE of 19.49 and the parametrized model was not able to follow accurately the measured voltage curve, as it is seen from Fig. 12. This deriving of the non-representative parameters can be caused by considering too short time period of the pulse, as it might not sufficiently represent the battery dynamics.

The most accurate results were obtained for the technique PT2, especially after the optimization, as it reached only 0.62 SSE. Both PT2 and PT3 followed accurately voltage dynamics during the relaxation period. However during discharging periods, the model is not able to follow very accurately the measured battery voltage. This comes from the fact that the parametrization was performed only from the relaxation period and did not consider the battery dynamics under operation, where dynamics might be different.

The extracted parameters from the PT2 (resistances, capacitances) have a strong relationship with the character of the OCV profile (Fig. 8) and the discharging voltage profile (Fig. 1). The capacitances' curves are copying directly their shapes and the resistances' curves have an inverse character. That might be seen as a confirmation of the correctness of the derived parameters.

VII. Conclusions And Future Work

In this work, measurement and parametrization techniques for deriving ECM parameters were presented. Afterward, the GITT was performed on the Li-S cell. The parameters for the ECM and the OCV for battery discharging were derived from the relaxation period of the voltage and from the discharging pulses.

The parametrized ECM was simulated with the same current profile as during battery laboratory measurement. The best accuracy has the model parameterized based on PT2. The simulated voltage was able to follow accurately the measured voltage with a SSE of 0.62. Therefore, the ECM for the Li-S battery was established for discharging GITT profile by 0.2 C under the temperature conditions of 35° C.

Future work will target the improvement of the parametrization technique in order to obtain a model which estimates more accurately the battery voltage during charging and discharging. The dependencies on the operating conditions, as temperature and current, can be included to the model. Such model should be also validated against different current profiles.

Acknowledgment

References

[1] D. Bresser, S. Passerini, and B. Scrosati, "Recent progress and remaining challenges in sulfur-based lithium secondary batteries - a review," *Chem. Commun.*, vol. 49, no. 90, pp. 10 545–10 562, Nov. 2013.

[2] X. Hu, S. Li, and H. Peng, "A comparative study of equivalent circuit models for Li-ion batteries," *J. Power Sources*, vol. 198, no. 0, pp. 359 – 367, 2012.

[3] A. Seaman, T.-S. Dao, and J. McPhee, "A survey of mathematics-based equivalent-circuit and electrochemical battery models for hybrid and electric vehicle simulation," *J. Power Sources*, vol. 256, pp. 410–423, Jun. 2014.

[4] M. Einhorn, F. V. Conte *et al.*, "Comparison, selection, and parameterization of electrical battery models for automotive applications," *IEEE Trans. Power Electron.*, vol. 28, no. 3, pp. 1429–1437, 2013.

[5] E. Barsoukov and J. R. Macdonald, *Impedance Spectroscopy Theory, Experiment, and Applications*, 2nd ed. John Wiley & Sons, Inc., 2005.

[6] "Program Battery Test Manual For Plug-In Hybrid Electric Vehicles," U. S. Department of Energy Vehicle Technologies, Tech. Rep., 2014.

[7] A. Hentunen, T. Lehmuspelto, and J. Suomela, "Time-Domain Parameter Extraction Method for Thévenin-Equivalent Circuit Battery Models," *IEEE Trans. Energy Convers.*, vol. 29, no. 3, pp. 558–566, 2014.

[8] "FreedomCAR Battery Test Manual For Power-Assist Hybrid Electric Vehicles," Idaho National Engineering & Environmental Laboratory (INEEL), Tech. Rep., October 2003.

[9] M. Daowd, N. Omar *et al.*, "Battery Models Parameter Estimation based on Matlab / Simulink ," in *The 25th World Battery, Hybrid and Fuel Cell Electric Vehicle Symposium & Exhibition Battery*, 2010.

[10] S. Thanagasundram, R. Arunachala, K. Makinejad *et al.*, "A Cell Level Model for Battery Simulation," *EEVC*, no. November, pp. 1–13, 2012.

[11] X. Lin, H. E. Perez, S. Mohan *et al.*, "A lumped-parameter electro-thermal model for cylindrical batteries," *J. Power Sources*, vol. 257, pp. 1–11, Jul. 2014.

[12] D. Liu, Z. Zhu *et al.*, "Parameter Identification of Improved Equivalent Circuits for Lithium-Ion Battery," *JCIT*, vol. 8, no. 5, pp. 1154–1162, Mar. 2013.

[13] X.-s. Hu, F.-c. Sun, and Y. Zou, "Online model identification of lithium-ion battery for electric vehicles," *J Cent South Univ T*, vol. 18, no. 5, pp. 1525–1531, 2011.

[14] X.-s. Hu, F.-c. Sun, and X.-m. Cheng, "Recursive calibration for a lithium iron phosphate battery for electric vehicles using extended Kalman filtering," *J Zhejiang Univ Sci A*, vol. 12, no. 11, pp. 818–825, 2011.

[15] Z. Deng, Z. Zhang *et al.*, "Electrochemical Impedance Spectroscopy Study of a Lithium/Sulfur Battery: Modeling and Analysis of Capacity Fading," *J. Electrochem. Soc.*, vol. 160, no. 4, pp. A553–A558, Jan. 2013.

[16] N. a. Cañas, K. Hirose, B. Pascucci *et al.*, "Investigations of lithium-sulfur batteries using electrochemical impedance spectroscopy," *Electrochim. Acta*, vol. 97, pp. 42–51, May 2013.

[17] K. Somasundaram, O. Neill, M. Marinescu *et al.*, "Towards an operational model for a Li-S battery," Poster, London, Sep. 2014.

[18] M. Barghamadi, A. Kapoor, and C. Wen, "A Review on Li-S Batteries as a High Efficiency Rechargeable Lithium Battery," *J. Electrochem. Soc.*, vol. 160, no. 8, pp. A1256–A1263, May 2013.

[19] V. Kolosnitsyn, E. Kuzmina *et al.*, "A study of the electrochemical processes in lithiumsulphur cells by impedance spectroscopy," *J. Power Sources*, vol. 196, no. 3, pp. 1478–1482, Feb. 2011.

[20] C. Barchasz, J.-C. Leprêtre *et al.*, "New insights into the limiting parameters of the Li/S rechargeable cell," *J. Power Sources*, vol. 199, pp. 322–330, Feb. 2012.

[21] V. Kolosnitsyn, E. Kuzmina, and S. Mochalov, "Determination of lithium sulphur batteries internal resistance by the pulsed method during galvanostatic cycling," *J. Power Sources*, vol. 252, pp. 28–34, Apr. 2014.

[22] E. Karden, "Using low-frequency impedance spectroscopy for characterization, monitoring, and modeling," Ph.D. dissertation, RWTH Aachen University, 2002.

[23] H. G. Schweiger, O. Obeidi, O. Komesker *et al.*, "Comparison of several methods for determining the internal resistance of lithium ion cells," *Sensors*, vol. 10, pp. 5604–5625, 2010.

[24] W. Weppner and R. A. Huggins, "Determination of the Kinetic Parameters of Mixed-Conducting Electrodes and Application to the System Li_3Sb," *J. Electrochem. Soc.*, vol. 124, no. 10, pp. 1569–1578, 1977.

[25] R. Jackey, M. Saginaw, P. Sanghvi *et al.*, "Battery Model Parameter Estimation Using a Layered Technique: An Example Using a Lithium Iron Phosphate Cell Pulse Tests to Measure Dynamic," pp. 1–14, 2013.

[26] H. He, R. Xiong, and J. Fan, "Evaluation of Lithium-Ion Battery Equivalent Circuit Models for State of Charge Estimation by an Experimental Approach," *Energies*, vol. 4, no. 12, pp. 582–598, Mar. 2011.